

2-1-3 Structure of Interplanetary Magnetic Cloud Estimated by Fitting Magnetic Flux Rope Models

ISHIBASHI Hiromitsu

We examined the relationship between interplanetary magnetic cloud observed by the ACE satellite on April 16, 1999 and its solar origin. The solar and interplanetary background was relatively quiet for 10 clear days before April 16, enabling us to unambiguously assume the solar origin of the magnetic cloud. However, the results of fitting a constant-alpha force-free cylindrical flux rope model is inconsistent with findings from previous studies about magnetic clouds and their solar origins, although corresponding solar surface phenomena occurred near the central meridian. We therefore attempted to fit another model with the torus-shaped magnetic field structure, which is a simple extension of the conventional cylindrical model with more geometrical flexibility. Using the estimated planar structure of the flux rope, we were able to interpret reasonably the observed magnetic cloud as an expansion into interplanetary space of a filament eruption or halo CME (coronal mass ejection) on April 13, 1999.

Keywords

Interplanetary magnetic flux rope, Solar wind, Interplanetary magnetic field, Coronal mass ejection, Disappearing solar filament

1 Introduction

Among the sudden solar surface phenomena, coronal mass ejection (CME) is being elucidated in detail through high-resolution observations using the SOHO, TRACE, and other artificial satellites. However, studies on CME in interplanetary space covering a distance of more than 30 times the sun's radius (R_s) and on interplanetary CME (ICME) depend on in-situ observation with exploratory spacecrafts scattered in the vast interplanetary space; therefore, the space structure and propagation characteristics of CME have yet to be well clarified. In addition, ICME is considered to undergo changes in its structure and propagation velocity due to the interaction with background solar winds during its propagation process, thereby making it even more difficult to elucidate. Attempts to identify the charac-

teristics of plasma and magnetic fields in ICME were made during the first years of solar wind observation, and the most widely known characteristics are: (1) a bidirectional flow of high-temperature electrons, (2) an abnormally low proton temperature, and (3) a magnetic field structure with twisted magnetic lines called magnetic flux ropes [1]–[3]. Both the modeling and method of analyzing magnetic flux ropes have benefited from many enhancements through gradual development following a trial description of the characteristic magnetic field changes in magnetic flux ropes as evidenced in observational data by using a cylindrical magnetic flux rope model (Fig. 1) based on the Lindquist solution for an axisymmetric force-free magnetic field. These study results have also greatly contributed to attempts at elucidating the cause-and-effect relationship between solar surface phenomena

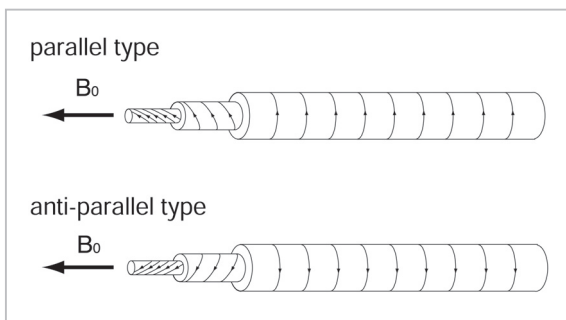


Fig. 1 Geometrical configuration of the cylindrical magnetic flux rope

and the generation of magnetic field flux ropes, which are closely related to ICME, such as coronal arcade formation, prominence eruptions, and disappearing solar filament (DSF)[4]–[8]. In other words, this technique involves fitting the magnetic flux rope model to IMF observational data, thereby estimating the geometrical and physical parameters of a magnetic flux rope, and, based on those parameters, going back to the sun and exploring the sources thereof in an attempt to validate the physical harmony with related solar surface phenomena. Above all, a sudden solar surface phenomenon occurring in isolation after both the sun and interplanetary space have remained quiet for several days makes it possible to track a series of phenomena from the solar surface to the proximity of the earth, including DSF and other solar surface phenomena, CME, ICME near IAU, and other geomagnetic disturbances. And since such tracking allows us to identify their cause-and-effect relationships in a relatively easy manner, these events will also be suitable for considering the appropriateness of the magnetic flux rope model. This paper introduces an analysis conducted on a series of phenomena that occurred due to the DSF event on April 13, 1999, by using a force-free magnetic field flux rope model. Although the filament located in the middle of the solar surface directly facing the earth disappeared in this event, an estimate based on cylindrical magnetic rope indicated a result conflicting with the law governing the relationship between the solar surface magnetic field near the filament found

in previous studies on one hand, and the magnetic flux rope in a magnetic cloud on the other[4][5]. However, the cylindrical model is a very simplified one and, depending on the positional relation between ICME and a satellite, the curvature of the magnetic flux rope will become an important factor and the cylindrical model may not constitute an appropriate approximation. A torus-shaped magnetic flux rope model based on a circularly bent cylinder is therefore an effective means in such cases[3][5]. This paper briefly introduces an overview of a series of phenomena stemming from the DSF event that occurred on April 13, 1999. It then describes the relation between the magnetic flux rope structure and the corresponding solar surface phenomena as estimated based on the fitting results of the cylindrical magnetic rope model and torus-shaped rope model.

2 Observation

At around 10:30 (UT) on April 16, 1999, the ACE satellite observed a passing shock wave. Immediately after the shock wave passed, there was a dramatic increase in solar wind density, which reached a peak of 68 atoms per cubic centimeter at around 14:00 (UT) on the same day. In continuation, the magnetic field began turning southward at around 21:00 (UT) in the evening, reaching a peak of -13 nT. The duration of $B_z < -10$ nT lasted about six hours. Then at 11:26 (UT), an SC-type geomagnetic storm occurred and ended around 17:21 (UT). The maximum decline in the horizontal component of geomagnetism observed at Kakioka was about 160 nT.

To ensure correspondence with solar surface phenomena, SOHO/LASCO EIT195 data was tracked for several days before the shock wave passed, in order to identify active phenomena on the solar surface. There was low solar activity during that period with the interplanetary space remaining relatively quiet, so that the only candidate phenomenon identified was the halo CME observed by LASCO/C2 at

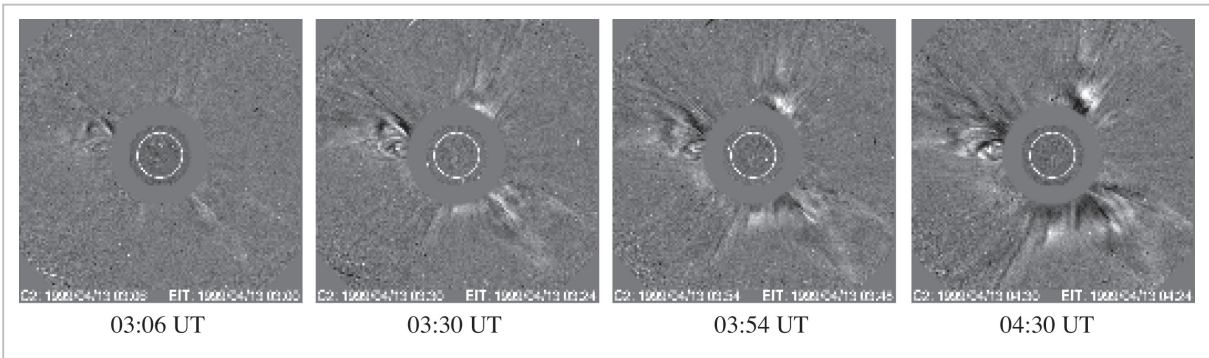


Fig.2 Halo CME observed with a LASCO C2 coronagraph on April 13, 1999

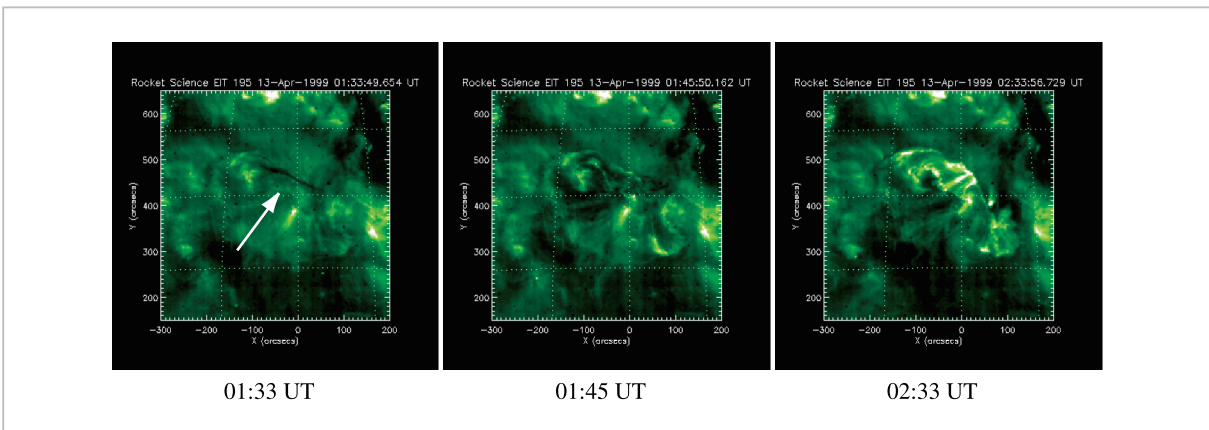


Fig.3 Observation by SOHO/EIT 195Å on April 13, 1999

From the far left in the figure: the filament near the meridian of the Northern Hemisphere (the white-line arrow), the decline (dimming) in coronal brightness near the filament, and formation of the arcade structure

around 03:30 (UT) on April 13 (Fig. 2).

A CME corresponding to a small X-ray flare was also observed at around 10:00 (UT) on the same day, but since its source was in the southeastern part with the CME apparently occurring on the eastern side, the event was unlikely to affect the space environment near the earth. Moreover, observations by EIT195 showed a decline (dimming) in coronal brightness at around 01:48 (UT) near the filament in the middle of the Northern Hemisphere prior to that halo CME, followed by the formation of an arcade structure at around 02:30 (UT) (Fig. 3).

H α ray observation in a Meudon spectroheliogram also confirmed this disappearing solar filament (N16E00) in observations taken at 20:34 (UT) on April 12 and at 10:58 (UT) on April 13 (Fig. 4).

Moreover, the solar radio observation sys-

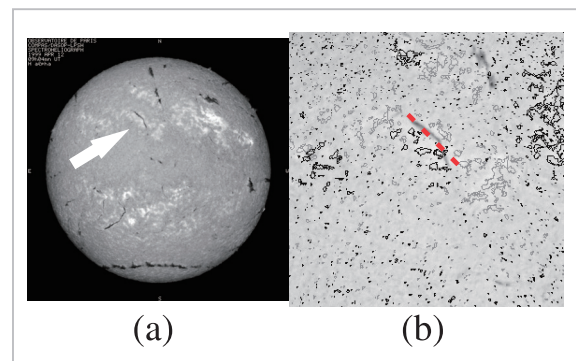


Fig.4 (a) H-alpha image on a Meudon heliograph on April 12, 1999. The filament indicated with the white arrow disappeared. (b) The figure of the H-alpha image from (a) overlapped with contours of the SOHO/MDI magnetoheliogram

(Gray: positive polarity; black: negative polarity)
The red dotted line indicates the approximate direction of the filament as extended northeast to southwest on the center line of the magnetic field on the solar surface.

tem (HiRAS) of NICT's Hiraiso Solar Observatory also observed a weak type IV radio burst around 03:00 (UT) on the same day. Both events are presumably closely related to the occurrence of CME [9][10]. We therefore considered it appropriate to conclude that the source of ICME that passed the ACE satellite on the 16th was in the DSF generated with the halo CME on April 13.

3 Fitting with a magnetic flux rope model

3.1 Cylindrical magnetic flux rope model

A magnetic flux rope model is applied to changes in the magnetic fields of the solar winds in events described in the preceding chapter, in order to determine the model's direction and size, the magnitude of the main magnetic field, and other parameters. The cylindrical magnetic flux rope model described in a constant- α force-free magnetic field that self-expands in a similar manner is well recognized and enjoys widespread use as a model that briefly and rationally explains the twisted magnetic field structure in ICME [5][11]. Therefore, fitting was initially conducted by using a cylindrical magnetic flux rope model to verify the relation between ICME and DSF.

As a result of the fitting, the direction of main magnetic field of the magnetic rope expressed by geocentric solar ecliptic coordinates as the standard becomes as follows: latitudinal angle θ and longitudinal angle ψ become -40.0° and 120.2° , respectively.

The helicity of magnetic lines in the magnetic rope is left-handed (antiparallel).

The other estimated parameters are as follows:

Radius of the magnetic flux rope: 0.102 AU
Intensity of the main magnetic field: 25.2 nT
Collision parameter: 0.29

where, the collision parameter is the distance between the satellite orbit's and the axis of the magnetic rope as standardized by its radius.

A study of the relation between magnetic flux ropes and troidal magnetic fields in the solar winds [4] and an analysis of the structure of the filament magnetic field [8] have revealed that the helicity of magnetic flux stemming from the Northern Hemisphere has a left-handed (antiparallel) magnetic field structure, while that stemming from the Southern Hemisphere has a right-handed (parallel) one. This theory leads us to conclude that this magnetic flux rope originated in the Northern Hemisphere. In other words, this conclusion supports the concept of this magnetic flux rope event having originated in the DSF that occurred on the 13th. The observation of magnetic fields on the solar surface by SOHO/MDI reveal that the magnetic field near the filament in question is oriented vertically upwards north of the filament and vertically downwards to the south. Assuming that the filament with left-handed (antiparallel) magnetic helicity had already been released into interplanetary space, then reasonable explanations can be given about the twisted structure of the magnetic field in the magnetic flux rope estimated by fitting the ACE satellite observations based on surface magnetic field observations and the cylindrical magnetic rope model based on SOHO/MDI [6][12].

Recent studies conducted on magnetic helicity (left-handed) have yielded results not contradicting past studies that considered magnetic flux ropes to have originated in solar surface phenomena, though the main magnetic field vector of magnetic flux rope projected on the Y-Z plane in the GSE coordinate system is almost in the northwest to southeast direction (to -45.1°) and almost perpendicular to the direction of the filament in question (Fig. 4). Accepting this analysis result entails assuming that the direction of the magnetic flux rope was significantly changed during its propagation through interplanetary space. For these reasons, although the DSF occurred nearly in front and directly facing the earth, fitting with the cylindrical magnetic flux rope model did not produce favorable results. Using this technique to determine the magnetic rope structure

essentially depends on the model and largely affects the estimated geographic relationship between the magnetic flux rope and filament [13]. One possible cause produced by the model itself is that a portion away from the middle of the magnetic flux rope passed the satellite, thereby explaining why the local description of the magnetic field structure based on the cylindrical magnetic flux rope model did not produce a good approximation, and adversely affecting the fitting results. To eliminate such effects, we attempted to conduct the fitting based on a torus-shaped magnetic flux model [5] with consideration given to curvature of the magnetic flux rope.

3.2 Torus-shaped magnetic flux rope model

Romashets and Vandas [14] devised a rigorous solution for the force-free magnetic field corresponding to a torus-shaped flux rope. This paper, however, employed a torus-shaped magnetic rope model [13] on an approximation solution [15] under conditions with the major radius of the torus sufficiently larger than its minor radius, thereby offering an even more simplified model where the mere fact that a magnetic rope has a circular axis also makes the inner magnetic field become a function of only distance from the main axis. In the torus-shaped magnetic flux rope model, the radius of a large circle expressed by the major radius of the torus (as an indicator of magnetic flux rope curvature) is added as a parameter, in addition to the thickness of the magnetic flux rope expressed with the minor radius of the torus. Moreover, the gradient of the entire torus with respect to the ecliptic is expressed as normal vectors (θn and ϕn) of the plane with the torus axis.

Figure 5 shows the fitting results of the ICME event obtained on April 16 and 17, 1999, as overlapped on the observational data. The figure shows the magnetic field intensity from above, the magnetic field X, Y, and Z components in the GSE coordinate system, solar wind velocity, proton density, temperature, β value, and the magnetic field vectors

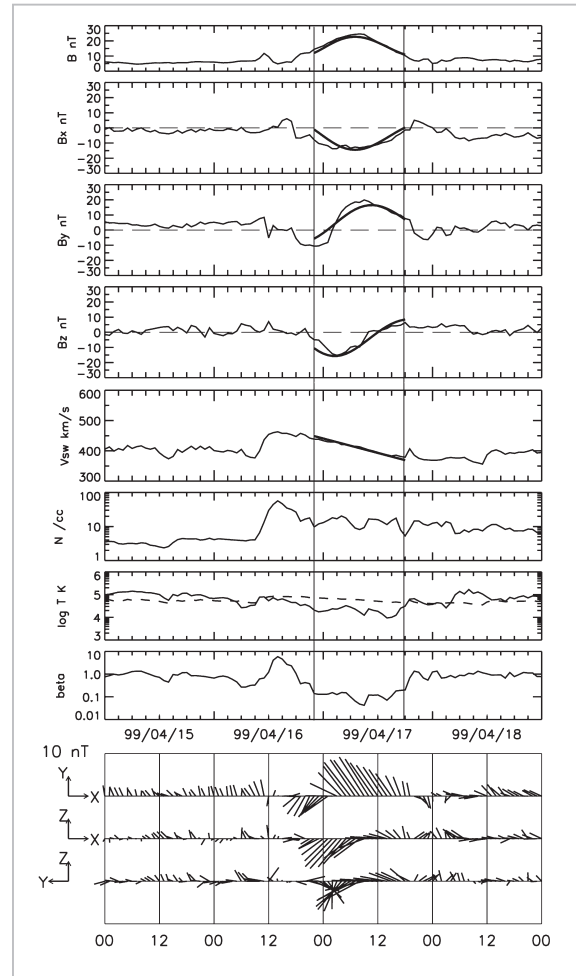


Fig.5 Magnetic flux rope event on April 16-17, 1999, where fitting was conducted with a torus-shaped model

From the top: magnetic field intensity, the magnetic field X, Y, and Z components in the GSE coordinate system, solar wind velocity, proton density, temperature, β value, and magnetic field vectors projected on the X-Y, X-Z, and Y-Z planes

projected on the X-Y, X-Z and Y-Z planes. The expected value taken from the relation between the solar wind velocity and proton temperature [16] is indicated by the dotted line in the figure for proton temperature, and used to identify the passage of a magnetic cloud based on a lower proton temperature than the expected value [2].

For the torus plane, θn and ψn have normal vectors of -18° and 33° , respectively, and like the fitting results based on the cylindrical model described above, the magnetic field

structure in the magnetic flux rope was left-handed (antiparallel). The other parameters obtained by the fitting are as follows:

Major radius of the torus:	0.3 AU
Minor radius of the torus:	0.07 AU
Main magnetic field intensity:	23 nT
Collision parameter P_y (GSE coordinate system, Y component):	-0.24
Collision parameter P_z (GSE coordinate system, Z component):	-0.21

Here, the collision parameters are the result of standardizing the distance between the satellite's orbit and magnetic rope along with its radius (minor radius of the torus).

The collision parameters P_y and P_z lead to an estimation whereby the center of the torus passed by south of the surface of the ecliptic.

In analysis conducted with a torus-shaped magnetic flux rope model, the magnetic flux rope is fitted as a part of the torus whose θ_n and ψ_n have normal vectors of -18° and 33° , respectively, and explained with a plot showing where the south end of the torus passed by the ACE satellite. Figure 6 is a geometric sketch of the magnetic flux rope obtained with this fitting.

The plane estimated based on a torus model with the torus axis tensioned is almost

along the Archimedes spiral. Another very important point is that the main magnetic field vector estimated based on the aforementioned cylindrical magnetic flux rope model is included in this torus plane. By assuming that a filament released along the magnetic neutral plane extending northeast to southwest with the DSF propagating through interplanetary space was observed as a magnetic flux rope having torus-shaped geometric characteristics along the Archimedes spiral in IAU, the series of events from the DSF to the magnetic flux rope observed by the ACE satellite can then be explained without contradictions.

4 Conclusion

This paper presented a cylindrical flux rope model and its developed version, a torus-shaped magnetic flux rope model obtained through fitting analysis of the magnetic flux rope event that occurred on April 16, 1999, based on a magnetic flux rope model. Attempts to establish the physical coordination between DSF, arcade structure, CME, and other solar surface phenomena on the one hand, and ICME on the other yielded important clues to learning about the temporal and spatial developmental process of magnetic clouds in interplanetary space, with the magnetic flux rope model having been enhanced and developed as an important analysis tool for that purpose. Analysis based on a cylindrical magnetic flux rope model has previously produced many cases of successful results relative to solar surface phenomena. For the event reported in this paper, the corresponding solar surface phenomena occurred almost on the meridian plane directly facing the earth, but failed to produce rational analysis results. However, the torus-shaped magnetic flux rope model resolved the problems regarding the cylindrical model with consideration given to the magnetic rope curvature, resulting in a reasonable explanation of the series of observed facts. In past studies, many ICME events failed to produce favorable results in fitting with a cylindrical model, so that revalidating

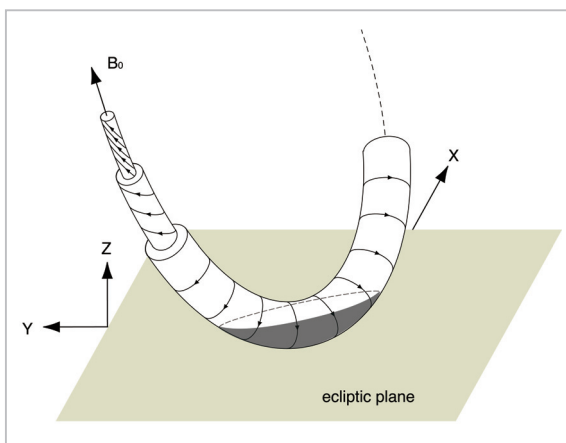


Fig.6 Schematic diagram of the coordination of a torus-shaped magnetic flux rope corresponding to the fitting results from Fig. 5

In the figure, the shaded portion comes below the surface of the ecliptic.

those events with a torus-shaped magnetic rope model could prove significant. Conversely, the scope of the fitting program must be expanded by proceeding with enhancement of the torus-shaped magnetic flux rope model itself from approximation solutions for the

applicable force-free magnetic field, to those based on rigorous solutions independent of the major and minor radii of the torus, assuming that the major radius of the torus used in this paper is sufficiently larger than its minor radius.

References

- 1 Gosling J. T., Baker D. N., Bame S. J., Feldman W. C., Zwickl R. D., and E. J. Smith, "Bidirectional solar wind electron heat flux events," *J. Geophys. Res.*, 92, 8519–8535, 1987.
- 2 Richardson, I. G. and H. V. Cane, "Regions of abnormally low proton temperature in the solar wind (1965–1991) and their association with ejecta," *J. Geophys. Res.*, 100, 23397, 1995.
- 3 Marubashi, K., "Physics of interplanetary magnetic flux ropes: toward prediction of geomagnetic storm," *Adv. Space Res.*, 26(1), 55–66, 2000.
- 4 Marubashi, K., "Structure of the interplanetary magnetic clouds and their origins," *Adv. Space Res.*, 6(6), 335–338, 1986.
- 5 Marubashi, K., "Interplanetary magnetic flux ropes and solar filaments, in Coronal Mass Ejections," *Geophys. Monogr. Ser.*, Vol. 99, edited by N. Crooker, J. Joselyn, and J. Feynman, p. 147, AGU, Washington, D.C., 1997.
- 6 Bothmer, V. and R. Schwenn, "Eruptive prominences as sources of magnetic clouds in the solar wind," *Space Sci. Rev.*, 70, 215–220, 1994.
- 7 Bothmer, V. and D. M. Rust, "The field configuration of magnetic clouds and solar cycle, in Coronal Mass Ejections," *Geophys. Monogr. Ser.*, Vol. 99, edited by N. Crooker, J. Joselyn, and J. Feynman, p. 139, AGU, Washington, D.C., 1997.
- 8 Rust, D. M., "Spawning and shedding helical magnetic fields in the solar atmosphere," *Geophys. Res. Lett.*, 21, 241–244, 1994.
- 9 Munro, R. H., J. T. Gosling, E. Hildner, R. M. MacQueen, A. Poland, and C. L. Ross, "The association of coronal mass ejection transients with others forms of solar activity," *Sol. Phys.*, 61, 201–215, 1979.
- 10 Webb, D. F. and A. J. Hundhausen, "Activity associated with the solar origin of coronal mass ejections," *Sol. Phys.*, 108, 383–401, 1987.
- 11 Farrugia, C. J., L. F. Burlaga, V. A. Oshrovič, I. G. Richardson, M. P. Freeman, R. P. Lepping, and A. J. Lezarus, "A study of an expanding interplanetary magnetic cloud and its interaction with the Earth's magnetosphere," *J. Geophys. Res.*, 98, 7621–7632, 1993
- 12 Rust, D. M. and A. Kumar, "Helical magnetic fields in filaments," *Sol. Phys.*, 155, 69, 1994.
- 13 Marubashi, K., "Interplanetary magnetic flux ropes," *J. Comm. Res. Lab.*, 49(3), 41–59, 2002.
- 14 Romashets, E. and M. Vandas, "Force-free field inside a toroidal magnetic cloud," *Geophys. Res. Lett.*, 30(20), 2065–2068, 2003.
- 15 Miller, G. and L. Turner, "Force free equilibria in toroidal geometry," *Phys. Fluids*, 24, 363–365, 1981.
- 16 Lopez, R., "Solar cycle invariance in solar wind proton temperature relationships," *J. Geophys. Res.*, 92, 11189, 1987.



ISHIBASHI Hiromitsu

*Senior Researcher, Space Environment
Group, Applied Electromagnetic
Research Center
Solar Wind, Space Weather*